Evanescent coupling of transmitted light through an array of holes in a metallic film assisted by transverse surface current

2003 J. Phys.: Condens. Matter 15 8147

(http://iopscience.iop.org/0953-8984/15/47/017)

INSTITUTE OF PHYSICS PUBLISHING JOURNAL OF PHYSICS: CONDENSED MATTER

J. Phys.: Condens. Matter **15** (2003) 8147–8156 PII: S0953-8984(03)67075-X

Evanescent coupling of transmitted light through an array of holes in a metallic film assisted by transverse surface current

Guo Ping Wang[1], **Yongxiang Yi and Bing Wang**

Department of Physics, Wuhan University, Wuhan 430072, People's Republic of China

E-mail: kp_wang@hotmail.com

Received 2 August 2003, in final form 30 September 2003
Published 14 November 2003
Online at stacks.iop.org/JPhysCM/15/8147

Abstract
The ultraordinary transmission of light through an array of holes in both perfect and real metallic films is simulated with the three-dimensional finite-difference time-domain method. We demonstrate that two distinguishing physical processes dominate the transmission behaviour: transverse surface current excited on the entrance surface of the metallic film transports light energy to the holes, while the evanescent coupling of incident and reflected waves inside the holes transmits light from the entrance to the exit of the holes. Surface plasmons excited on the flat parts of metallic hole arrays make a positive impact in the energy transportation of the first process, but are not necessary for the enhanced transmission. Our results are contrary to some recent theoretical results but agree with the experimental observations available.

1. Introduction

Spurred by numerous potential applications in photonics and optoelectronics, and the rich physics involved in itself, the experimental discovery of enhanced optical transmission of light through sub-wavelength hole arrays perforated in metallic films [1] provides increasing interest [2–14]. For insight into the physical origin of the transmission enhancement, one-dimensional (1D) metallic gratings with sub-wavelength slits are investigated intensively as an alternative model [2–8]. Although such 1D gratings exhibit some qualitative agreements with the hole arrays in a transmission spectrum, electromagnetic modes inside the slits of the 1D gratings are different from that of a hole array [8]. Therefore, a real two-dimensional (2D) model is crucial for fully understanding the mechanism behind the enhanced transmission. To date, surface plasmon (SP) assisted transmission [1, 11, 15], the tunnelling coupling

[1] Author to whom any correspondence should be addressed.

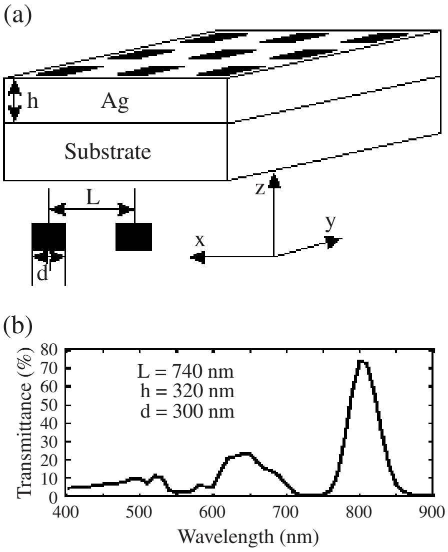

Figure 1. (a) Schematic view of the model for simulation. L, d, and h are the period of the hole array, the hole width, and the thickness of the metallic film, respectively. (b) Transmission spectrum of a square hole array in Ag film with $L = 740$ nm, $d = 300$ nm, and $h = 320$ nm, respectively.

effect [9, 10], and dynamic diffraction by the hole arrays [12, 13] are some representative points of view proposed to elucidate the physics of the ultraordinary transmission.

In our previous papers [7, 14], we have preliminarily confirmed that the enhanced transmission is due to TEM wave assisted F-P resonance in 1D gratings [5, 7] and surface current supported waveguide coupling in 2D hole arrays [4, 6, 14], respectively. This paper tries to give a more detailed physical scheme for better understanding of the enhanced transmission. In our analysis, the three-dimensional (3D) finite-difference time-domain (FDTD) method [16] is used for theoretical simulations. The method is a discrete straightforward calculation of Maxwell's equations and has previously been used to simulate the electromagnetic propagation of 1D slit gratings [7, 17] and 2D hole arrays in metallic films [14, 18], respectively. Based on numerical calculations, we argue that transverse surface current (TSC) excited on the entrance surface of a metallic film transports light energy to holes and then evanescent coupling inside the holes [10] transmits light from the entrance to the exit of the holes. We will also reveal that, instead of playing a negative role in optical transmission [6], SPs on the flat parts of metallic hole arrays play a positive role in the first transportation process.

2. Model and method

Figure 1(a) shows the model used to perform our simulations, in which a dielectric substrate supported metallic film (Ag) with a square hole array is considered. The array parameters are sketched in the figure. Dividing the computational domain into a series of cubic cells with edge-length $\Delta x = \Delta y = \Delta z = g$ along x, y, and z axes, and using N, $\Delta t = g/(2c)$ (c is the velocity of light), and (i, j, k) to denote the number and length of the time-steps, and the spatial position, respectively, we can write electromagnetic components E_X, E_Y, E_Z, H_X, H_Y, and H_Z at any spatial and temporal step t $(=N\Delta t)$ as F:

$$F^N(i, j, k) = F(i\Delta x, j\Delta y, k\Delta z, N\Delta t). \quad (1)$$

From the formula, Maxwell's equations are transformed into a series of discrete scalar ones. By solving equation (1), we can get the transmittance of light through a hole array in metallic films [7, 14]. The transmittance is defined as $\sum I_0/\sum I$, where $\sum I_0$ and $\sum I$ are the sum of $|\boldsymbol{E}|^2$ of incident and transmitted light over the illumination areas, respectively. In all the calculations, a plane wave normally illuminating the square hole arrays from the substrate side is assumed (z axis). On the top and bottom and other sides of the computational domain, a second absorption boundary condition [19] and a periodic boundary condition are used, respectively. The dielectric constant of the Ag film is obtained from [20], which has been used to yield the desired values of the dielectric constants at any frequencies by the best fitting method. The conductivities σ used are obtained from the imaginary part of the dielectric constants in terms of the Drude model. Figure 1(b) shows a calculated transmittance spectrum of TM-polarized ($H_z = 0$) light through a square hole array with similar structure parameters to that of [9]. The computational domain (a period of the hole array) is divided into $40 \times 40 \times 100$ cells with $g = 20$ nm. In this condition, the electromagnetic field distribution around the holes reaches a convergent state after 1500 time-steps ($N = 1500$, about 15 T; T is the oscillation period of the incident light). Using a Pentium IV personal computer with 1.5 GHz CPU and 512 Mbytes memory, with 10 nm wavelength-step, we get the transmittance spectrum with about 80 h CPU time after $N = 1600$. A good agreement with experimental measurement and the theoretical result obtained by another method (corresponding to figures 1 and 2 of [9], respectively) confirms the working of our computational program. Discrepancy between the calculated and the measured values can be attributed to the imperfect fabrication of the holes in experiment as pointed out by [9].

3. Results and discussion

Figure 2 presents the simulated transmittance of a TM-polarized wave through a hole array. The dielectric constant of the substrate and period of the hole array are chosen as $\varepsilon_s = 2$ and $L = 740$ nm, respectively. Other parameters are (a) $d = 300$ nm and $h = 360, 400$, and 600 nm and (b) $h = 320$ nm and $d = 220$, 260, and 300 nm, respectively. The results show strong transmittance peaks at wavelengths much longer than the hole size. Normalizing the peak transmittances by hole area of the array, one can find an unusual transmission enhancement at the peak wavelengths. For instance, with $d = 300$ nm, when h is set at 320 nm, the transmittance around $\lambda = 800$ nm reaches about 74%, while the filling fraction of the hole area on the film surface is 16.4%. As a result, an enhancement factor of 4.5 is obtained (figure 2(b), bottom). As film thickness, or hole depth, increases, the transmittance will decrease but shows no spectral shift (figure 2(a)). When the hole depth becomes too deep to some extent, transmittance peaks will disappear and no transmission enhancement occurs. This is completely different from the case of a 1D metallic grating with sub-wavelength slits. In the 1D case, transmittance peaks show no decrease with increasing film thickness [3, 5, 7, 8]. On the other hand, with a fixed hole depth, similar to the report of [9], the transmittance peaks become stronger and show a slight red shift simultaneously as the hole width increases (figure 2(b)). Tunnelling coupling between surface electromagnetic modes on both sides of the metal film was proposed to explain the origin of the transmission phenomenon [9, 10].

Recently, Vigoureux [12] and Treacy [4, 13] attributed the extraordinary transmission to a pure diffraction of the hole array. However, experimental observation shows that such a hole array in a germanium (Ge) film exhibits no transmission enhancement [1] although diffraction still occurs. Considering that the free charge density of Ge (in the order of 10^{16} m^{-3} [21]) is much less than that of metals (aluminium, for example, 10^{29} m^{-3} [22]) and the amplitude of the surface current is proportional to the free charge density, we attribute energy transportation of

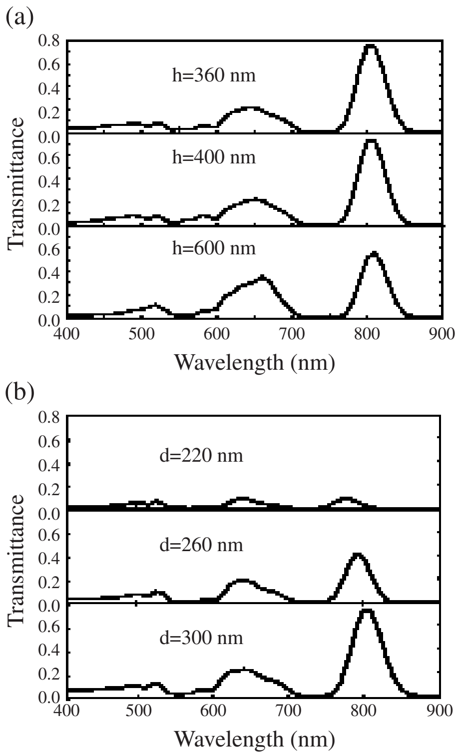

Figure 2. Transmission spectra of the square hole array with $L = 740$ nm in Ag film as a function of (a) h and (b) d, respectively. $d = 300$ nm in (a) and $h = 320$ nm in (b) are fixed, respectively.

the incident light to the holes to the surface electric field, known as surface current (SC) [4, 6]. The amplitude of SC in the Ge film induced by incident light is too small to couple enough energy into the holes and then to enhance the transmission [1]. What should be noted is that, in the case of 1D gratings with TE-polarized illuminating light (electric field along the slits), although light induced SC still exists, the transmittance shows no enhancement [7, 8]. By analysing the flow direction of the SC on the grating surface excited by TE- and TM-polarized waves, respectively, one can find that TM light produced SC is perpendicular to the slits (figure 3(a)), while TE light excited SC is parallel to the slits (figure 3(b)). The former can interact with the slits and transport light energy from the metallic surface to the slits but the latter cannot. Therefore, TM light may produce in the 1D metallic gratings an enhanced transmission at some special wavelengths (depending on the second physical process which will be discussed later). In the case of 2D hole arrays, SC excited by both TE and TM waves can transport light energy to the holes along different directions of the array plane (figures 3(c) and (d)), thus a metallic hole array exhibits a same enhanced transmission regardless of the polarization direction of illumination light. From the above analyses, we argue that the enhanced transmission of light through a metallic hole array should exactly be associated with TSC flowing in the direction of intersecting holes or slits [14], not just with the SC propagating in an arbitrary direction [4, 6]. The TSC on the entrance surface plays the role of transporting light energy from metallic surface to the holes.

To confirm this idea, we simulate the $|\boldsymbol{E}|^2$ distribution around a square hole array with a plane wave normally illuminating the arrays from the substrate side. Figure 4 shows the

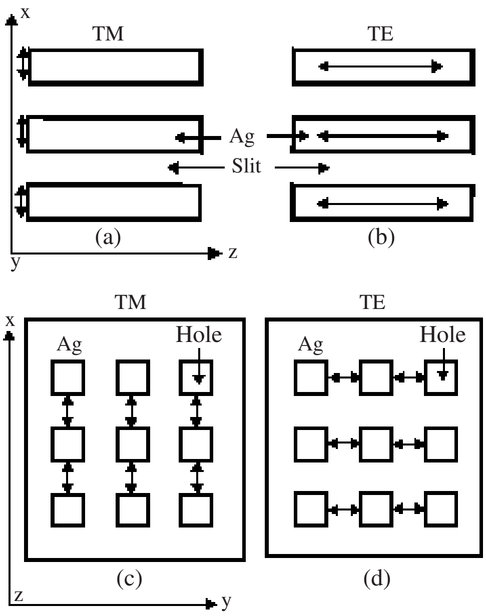

Figure 3. Schematic diagrams of SC direction on metallic film with (a), (b) slit and (c), (d) hole arrays, respectively. The incident light is along the z axis. $\leftrightarrow$ marks the direction of the SC.

sections of $|\boldsymbol{E}|^2$ in the y–z plane around a hole at different moments of 1 T–15 T, where $x = 0$ corresponds to a plane passing through the centre of the holes. Geometry parameters used for the simulation are $L = 740$ nm, $d = 300$ nm, and $h = 400$ nm. The light wavelengths (=800 nm (figure 4, left) and 730 nm (figure 4, right)) are with and without the enhanced transmission, respectively. The figures objectively display two main physical processes as light passes through the hole array: energy transportation from the film surface to the holes and coherent coupling of evanescent waves taking place inside the holes [9, 10]. When incident light illuminates the perforated metallic film, TSC on the entrance surface is excited and propagates along the surface. By scattering of the holes, the TSC transfers its energy into evanescent waves and then the evanescent waves propagate along the holes (figure 4(a)). As time elapses, the evanescent waves reach the exit of the holes and then are reflected by the exit surface [9, 10]. Both the reflected and original waves interfere with each other in the holes. The interference modulates the field distribution of the holes and further that of the entrance surface, and makes $|\boldsymbol{E}|^2$ at the entrance of the holes stronger and stronger (figures 4(b)–(e)). A more detailed simulation of the dynamics of this process in the time domain can clearly display the evolution of the coupling inside the hole array and the effect of the coupling on electric field intensities of both the entrance and exit surfaces. After several repeat processes of such coherent coupling, a steady-state field distribution at the exit of the holes is built up. The constructed coupling produces at the exit a stronger $|\boldsymbol{E}|^2$ ($\lambda = 800$ nm, figure 4(e), left) while a deconstructed coupling a weaker one ($\lambda = 730$ nm, figure 4(e), right). With a section at $y = 0$ of the y-axis, the $|\boldsymbol{E}|^2$ distribution in the x–z plane around the holes shows different pictures at local spots (not shown here). This can be attributed to the polarization direction of the illuminating light. Furthermore, in other y–z (x–z) planes at x (y) $\neq 0$, the local distribution pictures are also different, but a similar physical process is still deducible.

We would like to further stress here that, although SC [4, 6] was previously proposed to elucidate the enhanced transmission, TE-polarized light produced 1D slit gratings a flat

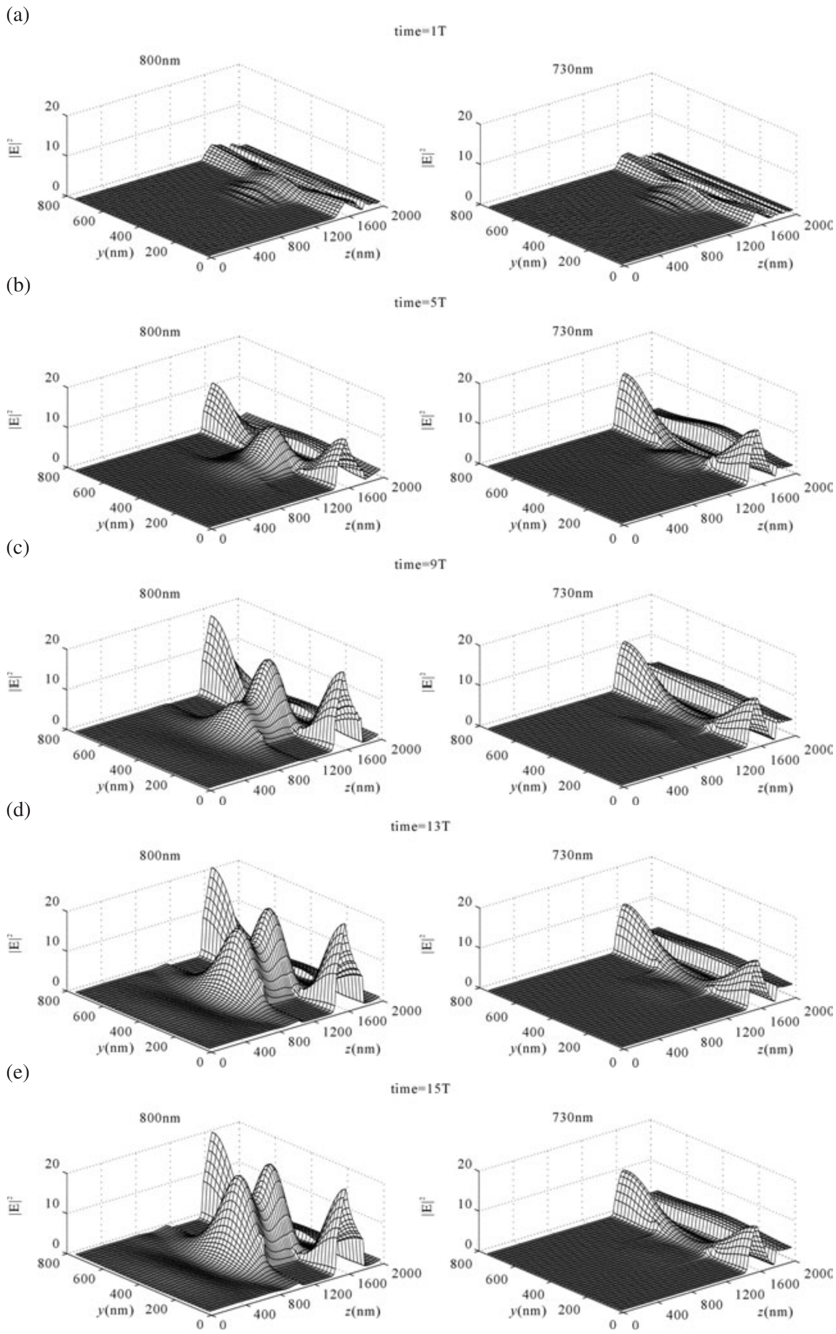

Figure 4. Sections of $|\boldsymbol{E}|^2$ distribution in the y–z plane at different moments around the holes of an array in Ag film with $L = 740$ nm, $d = 300$ nm (from $y = 250$ to 550 nm), and $h = 400$ nm (from $z = 1200$ to 1600 nm), respectively. Left, $\lambda = 800$ nm, and right, $\lambda = 730$ nm, are with and without the enhanced transmission, respectively.

transmittance spectrum (no enhancement) reveals that TSC assisted resonance coupling should be more exact for the extraordinary transmission.

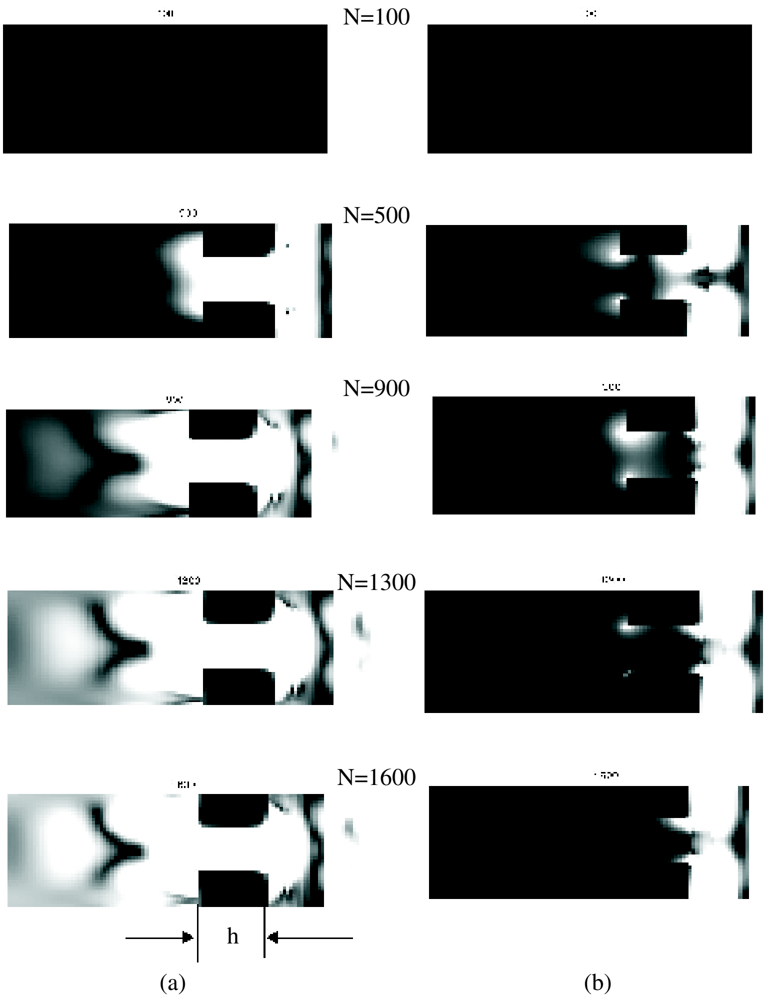

Figure 5. Near-field time evolution of the light through a hole array in a Ag film. λ = (a) 800 nm and (b) 730 nm are with and without the enhanced transmission, respectively. The array parameters are L = 740 nm, d = 300 nm, and h = 320 nm, respectively. The numbers 100, 500, ... denote the numbers N of the elapsed time-steps. The illuminated plane wave is incident from the right to the left.

Figure 5 shows the grey images of $|\boldsymbol{E}|^2$ around holes at the moments of $t = 100\Delta t$ to $1600\Delta t$ as a continuous plane wave normally passes through the square hole arrays from the substrate side, which cover the whole processes of the electrical field from the transient to the steady state ($t \geqslant 1500\Delta t$). It more clearly displays the effect of constructed ($\lambda = 800$ nm, figure 5(a)) and deconstructed coupling ($\lambda = 730$ nm, figure 5(b)) on field intensities around the holes. By second scattering at the exit of holes, the evanescent waves reradiate into the propagating modes [1, 9, 10]. As a result, an enhanced or flat transmission at different wavelengths appears in the far-field transmittance spectrum.

Concerning the peak shift of the transmission spectrum with hole size (figure 2(b)), we ascribe this to an evanescent waveguide effect. It is known that, in the case of a perfect metallic waveguide, the propagation coefficient γ of the electromagnetic modes along a square

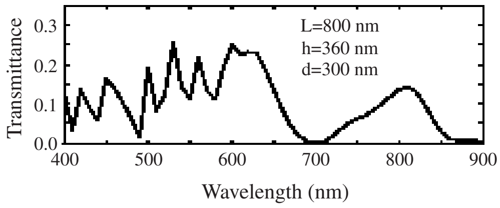

Figure 6. Transmission spectrum of a square hole array in a perfect metallic film with the same structure parameters as those of figure 2(a) (top) except $L = 800$ nm.

waveguide satisfies $\gamma^2 = \varepsilon\mu\omega^2 - 2(m\pi/d)^2$ [23] ($\gamma^2 < 0$, in our cases), in which m is an integer and ε and μ are the dielectric constant and permeability of the medium in the waveguide, respectively. One can see that, with a given propagation distance ($1/\mathrm{Im}[\gamma]$) [8] (here the hole depth), a larger hole size (bigger d) involves lower-frequency modes. Thus the transmission spectrum shows a red shift with increasing hole size. On the other hand, with a fixed hole dimension, optical modes involved in the holes are determined completely. The spectrum positions hence remain unchanged but the transmittance decreases with an increased hole depth due to the propagation loss (figure 2(a)). In contrast, in the slits of a 1D grating, there exist TEM modes, which have no cut-off wavelength and can constitute a channel for light to propagate normally [8]. Thus a 1D grating shows an enhanced transmission at longer wavelengths (for example, $\lambda > 3$ μm) even if the metallic film is very thick ($h = 4$ μm) [3, 5–8]. As a hole array structure, however, such a thick film will quench any transmission at wavelengths much longer than the cut-off wavelength of the holes [1]. In the case of a real metallic waveguide (Ag), the skin depth of the electromagnetic field in the metal will modulate the above waveguide dispersion relation and enhance the effective waveguide size. As a result, the real metallic waveguides will have a larger propagation coefficient γ than their perfect counterparts and hence have stronger transmittance [8].

Recently, Cao and Lalanne [6] stated that SPs play a negative role in light passing through a 1D metallic slit array. To make clear the role of SPs excited on the flat parts of the metallic surface of 2D hole arrays, we show in figure 6 the calculated transmittance of a hole array in a perfect metallic film with the same parameters as that of figure 2(a) (top) except $L = 800$ nm. The transmittance peak at $\lambda \approx 800$ nm is about 14.8% and correspondingly, the enhancement factor is 1.1, while in the Ag film case (figure 2(a), top) the enhancement factor reaches 4.6 at $\lambda \approx 800$ nm, which is with an excited SP mode on the flat parts of Ag hole arrays [1, 10, 24]. Considering that the skin depth of the electromagnetic field in the Ag film (about 24 nm around $\lambda \approx 800$ nm [24]) may modulate the effective waveguide size of the hole arrays and hence enhance the transmittance [8], we simply modify the filling fraction of the hole area on the film surface from the previous 16.4% ($d = 300$ nm) to the present 22.1% ($d = 348$ nm); a formatted enhancement factor of about 3.35 (much larger than 1.1) is also obtained. As has been stated before, if there is no energy transportation from the flat metallic surface to the holes, there will be no enhanced transmission. This implies that, although not a key factor, SPs excited on flat parts of a real metallic hole arrays are helpful for transporting much more energy to the holes. The conclusion means that, by proper design, a real metallic structure ($\mathrm{Im}(\varepsilon) \neq 0$) can impress its intrinsic damping to get stronger transmittance in the selected spectral region. This is in agreement with previous reports [5, 7, 8, 14]. But the effect of SPs made on the transmission properties of the hole array structures perforated in different metallic films may show special characteristics due to the variations of dielectric functions [10, 11]. A detailed comparison of such an effect among Au, Ag, and Al structures is in progress.

It should be noted that, in our simulations, the edge-length of each FDTD cell is set at $g = 20$ nm. This is close to the skin depth of the electromagnetic field in an Ag film of about 24 nm at the interesting wavelength and may be thought to have a negative influence on the calculated results. Nevertheless, our further calculation shows that, even with a edge-length $g = 6$ nm (much shorter than 24 nm), we also obtain a similar transmittance of the Ag hole array at around $\lambda \approx 800$ nm. Because of too long machine time, we could not show here the transmission spectrum of the 2D hole array in a larger spectrum range, but the fact that our FDTD simulations with cell length of $g = 6$ and 20 nm, respectively, on a 1D Ag grating show almost the same transmission spectrum in the range from the visible to near infrared confirms that the cell length $g = 20$ nm used in our simulations may have little influence on the resultant conclusions.

4. Conclusion

In conclusion, by the simulations of a plane wave through 2D sub-wavelength square hole arrays perforated in both perfect and real metallic films using the 3D FDTD method, we have proposed different physical processes to understand the transmission behaviour: TSC excited on the entrance surface of metallic films transports light energy from the film surface to the holes firstly, then evanescent coupling of the waves in the holes transmits light energy from the entrance to the exit. A constructed coupling in the holes results in an enhanced transmission. SPs excited on the flat surface of a real metallic hole array play a positive role in the process of energy transportation, but are not necessary for the enhanced transmission. Our conclusion should be interesting for better understanding the localization and coupling of electromagnetic field in metallic nanostructures as well as for optimizing modulation on the light field of active microstructures for biotechnology and so on.

Acknowledgments

We would like to thank the referees for their valuable comments, which have in part been cited in the paper. We also would like to acknowledge Wuhan University, Ministry of Education, and the National Natural Science Foundation (grant No. 60278018) of China for financial support.

References

[1] Ebbesen T W, Lezec H J, Gaemi H F, Thio T and Wolff P A 1998 *Nature* **391** 667
[2] Schröter U and Heitmann D 1998 *Phys. Rev.* B **58** 15419
[3] Porto J A, Garcia-Vidal F J and Pendry J B 1999 *Phys. Rev. Lett.* **83** 2845
[4] Treacy M M 1999 *Appl. Phys. Lett.* **75** 606
[5] Takakura Y 2001 *Phys. Rev. Lett.* **86** 5602
[6] Cao Q and Lalanne Ph 2002 *Phys. Rev. Lett.* **88** 057403
[7] Tan C, Yi Y and Wang G P 2002 *Acta Phys. Sin.* **51** 1063
[8] Popov E, Neviere E S and Reinisch 2000 *Phys. Rev.* B **62** 16100
[9] Martín-Moreno L, Garcia-Vidal F J, Lezec H J, Pellerin K M, Thio T, Pendry J B and Ebbesen T W 2001 *Phys. Rev. Lett.* **86** 1114
[10] Krishnan A, Thio T, Kim T J, Lezec H J, Ebbesen T W, Wolff P A, Pendry J, Martín-Moreno L and Garcia-Vidal F J 2001 *Opt. Commun.* **200** 1
[11] Wannemacher R 2001 *Opt. Commun.* **195** 107
[12] Vigoureux J M 2001 *Opt. Commun.* **198** 257
[13] Treacy M M J 2002 *Phys. Rev.* B **66** 195105
[14] Yi Y, Wang G P, Long Y and Shan H 2003 *Acta Phys. Sin.* **52** 604

[15] Salomon L, Grillot F, Zayats A V and de Fornel F 2001 *Phys. Rev. Lett.* **86** 1110
[16] Yee K K 1966 *IEEE Trans. Antennas Propag.* **14** 302
[17] Liu W-C and Tsai D P 2002 *Phys. Rev.* B **65** 155423
[18] Hohng S C, Yoon Y C, Kim D S, Malyarchuk V, Muller R, Lienau Ch, Park J W, Yoo K H, Kim J, Ryu H Y and Park Q H 2002 *Appl. Phys. Lett.* **81** 3239
[19] Mei K K and Fang J 1992 *IEEE Trans. Antennas Propag.* **40** 1001
[20] Palik E D 1985 *Handbook of Optical Constants of Solids* (Orlando, FL: Academic) pp 354–5
[21] Liu E, Zhu B and Luo J 1994 *Semiconductor Physics* (Beijing: National Defense Industry)
[22] Pendry J B, Holden A J, Stewart W J and Youngs I 1996 *Phys. Rev. Lett.* **76** 4773
[23] Jackson J D 1975 *Classical Electrodynamics* 2nd edn (New York: Wiley)
[24] Raether H 1988 *Surface Plasmons* (Berlin: Springer)